New Generation of Massless Dirac Fermions in Graphene under External Periodic Potentials

Cheol-Hwan Park,[1,2,*] Li Yang,[1,2] Young-Woo Son,[3,4] Marvin L. Cohen,[1,2] and Steven G. Louie[1,2]

[1]*Department of Physics, University of California at Berkeley, Berkeley, California 94720, USA*
[2]*Materials Sciences Division, Lawrence Berkeley National Laboratory, Berkeley, California 94720, USA*
[3]*Department of Physics, Konkuk University, Seoul 143-701, Korea*
[4]*School of Computational Sciences, Korea Institute for Advanced Study, Seoul 130-722, Korea*

(Received 24 June 2008; published 19 September 2008)

We show that new massless Dirac fermions are generated when a slowly varying periodic potential is applied to graphene. These quasiparticles, generated near the supercell Brillouin zone boundaries with anisotropic group velocity, are different from the original massless Dirac fermions. The quasiparticle wave vector (measured from the new Dirac point), the generalized pseudospin vector, and the group velocity are not collinear. We further show that with an appropriate periodic potential of triangular symmetry, there exists an energy window over which the only available states are these quasiparticles, thus providing a good system to probe experimentally the new massless Dirac fermions. The required parameters of external potentials are within the realm of laboratory conditions.

DOI: 10.1103/PhysRevLett.101.126804 PACS numbers: 73.61.Wp, 73.20.−r, 73.43.Lp, 73.50.Bk

Semiconducting and metallic superlattice structures are now routinely used in manipulating the electronic structure of materials [1]. These superlattices have additional electronic band gaps at the supercell Brillouin zone (SBZ) boundary, which often give rise to interesting phenomena.

Since the successful isolation of graphene [2–5], numerous studies have been performed on this novel material [6]. In particular, there have been a number of interesting theoretical predictions on graphene superlattices (defined to be graphene under an external periodic potential or graphene with periodic defects). For example, for a one-dimensional (1D) or a two-dimensional (2D) rectangular graphene superlattice, the group velocity of the low-energy charge carriers is renormalized anisotropically [7], a corrugated graphene sheet is expected to show charge inhomogeneity and localized states [8], and arrays of antidots (missing carbon atoms) of specific design could induce band gaps [9] or magnetism [10].

Graphene superlattices are not only of theoretical interest, but have also been experimentally realized. Superlattice patterns with a periodicity as small as 5 nm have been imprinted on graphene through electron-beam induced deposition of adatoms [11]. Also, triangular patterns with ~10 nm lattice period have been observed for graphene on metal surfaces [12–14]. Using periodically patterned gates is another possible route to make graphene superlattices.

In this Letter, we show that when a periodic potential is applied to graphene, a new generation of massless Dirac fermions is formed at the SBZ boundaries. The electronic wave vector (measured from the new Dirac point), the group velocity, and a *generalized* pseudospin vector, defined below, of the newly generated massless Dirac fermions are not collinear anymore. In 1D or 2D rectangular graphene superlattices, the features of these new massless Dirac fermions are obscured by other states existing around the new Dirac point energy. We show however that, in triangular graphene superlattices (TGSs), there can be no states other than those of the new massless Dirac fermions around the energy of the new Dirac points. Therefore, doped or gated TGSs should provide a clear way to probe this new class of massless Dirac fermions that are absent in pristine graphene.

A physical requirement for the discussed phenomenon is that the variation of the external periodic potential is much slower than the intercarbon distance so that intervalley scattering (between $\mathbf{K}$ and $\mathbf{K}'$) may be neglected [15,16], and we limit our discussion to the low-energy electronic states of graphene which have wave vectors close to the $\mathbf{K}$ point. The Hamiltonian of the low-energy quasiparticles in pristine graphene in a pseudospin basis, $\binom{1}{0}e^{i\mathbf{k}\cdot\mathbf{r}}$ and $\binom{0}{1}e^{i\mathbf{k}\cdot\mathbf{r}}$ [where $\binom{1}{0}$ and $\binom{0}{1}$ are Bloch sums of π orbitals with wave vector $\mathbf{K}$ on the sublattices A and B, respectively, and $\mathbf{k}$ is the wave vector from the $\mathbf{K}$ point], is given by [17]

$$H_0 = \hbar v_0(-i\sigma_x\partial_x - i\sigma_y\partial_y), \tag{1}$$

where v_0 is the group velocity and σ's are the Pauli matrices. The eigenstates and the energy eigenvalues are given by

$$\psi^0_{s,\mathbf{k}}(\mathbf{r}) = \frac{1}{\sqrt{2}}\begin{pmatrix} 1 \\ se^{i\theta_\mathbf{k}} \end{pmatrix} e^{i\mathbf{k}\cdot\mathbf{r}} \tag{2}$$

and

$$E^0_s(\mathbf{k}) = s\hbar v_0 k, \tag{3}$$

respectively, where $s = \pm 1$ is the band index and $\theta_\mathbf{k}$ is the polar angle of the wave vector $\mathbf{k}$. Equation (2) indicates that the pseudospin vector is parallel and antiparallel to the wave vector $\mathbf{k}$ in the upper band ($s = 1$) and in the lower band ($s = -1$), respectively. Moreover, the pseudospin vector is always parallel to the group velocity.

Let us first consider the case that a 1D potential $V(x)$, periodic along the x direction with periodicity L, is applied to graphene. The Hamiltonian H then reads

$$H = \hbar v_0(-i\sigma_x\partial_x - i\sigma_y\partial_y + IV(x)/\hbar v_0), \tag{4}$$

where I is the 2×2 identity matrix. After a similarity transformation, $H' = U_1^\dagger H U_1$, using the unitary matrix

$$U_1 = \frac{1}{\sqrt{2}}\begin{pmatrix} e^{-i\alpha(x)/2} & -e^{i\alpha(x)/2} \\ e^{-i\alpha(x)/2} & e^{i\alpha(x)/2} \end{pmatrix}, \tag{5}$$

where $\alpha(x)$ is given by [18]

$$\alpha(x) = 2\int_0^x V(x')dx'/\hbar v_0, \tag{6}$$

we obtain [19]

$$H' = \hbar v_0\begin{pmatrix} -i\partial_x & -e^{i\alpha(x)}\partial_y \\ e^{-i\alpha(x)}\partial_y & i\partial_x \end{pmatrix}. \tag{7}$$

To obtain the eigenstates and energy eigenspectrum of H' in general, using a plane wave spinor basis set, we need an infinite number of plane waves with wave vectors different from one another by the reciprocal lattice vectors of the superlattice. [A reciprocal vector of the superlattice is given by $\mathbf{G}_m = m(2\pi/L)\hat{x} \equiv mG_0\hat{x}$ where m is an integer.] However, if we are interested only in quasiparticle states whose wave vector $\mathbf{k} \equiv \mathbf{p} + \mathbf{G}_m/2$ is such that $|\mathbf{p}| \ll G_0$, we could treat the terms containing ∂_y in Eq. (7) as a perturbation since $\mathbf{G}_m$ is along $\hat{x}$. H' may be reduced to a 2×2 matrix using the following two states as basis functions

$$\begin{pmatrix} 1 \\ 0 \end{pmatrix}' e^{i(\mathbf{p}+\mathbf{G}_m/2)\cdot\mathbf{r}} \quad \text{and} \quad \begin{pmatrix} 0 \\ 1 \end{pmatrix}' e^{i(\mathbf{p}-\mathbf{G}_m/2)\cdot\mathbf{r}}. \tag{8}$$

[Note that the spinors $\binom{1}{0}'$ and $\binom{0}{1}'$ now have a different meaning from $\binom{1}{0}$ and $\binom{0}{1}$ that were defined before because of the unitary transformation.]

In order to calculate these matrix elements, we expand $e^{i\alpha(x)}$ as

$$e^{i\alpha(x)} = \sum_{l=-\infty}^{\infty} f_l[V]e^{ilG_0x}, \tag{9}$$

where $f_l[V]$'s are coefficients determined by the periodic potential $V(x)$. One important thing to note is that, in general,

$$|f_l| < 1, \tag{10}$$

which can directly be deduced from Eq. (9). The physics simplifies when the external potential $V(x)$ is an even function. Then, $f_l[V]$'s are all real [22]. For states with wave vector $\mathbf{k}$ very close to $\mathbf{G}_m/2$, the 2×2 matrix M whose elements are calculated from the Hamiltonian H' with the basis given by Eq. (8) can be written as

$$M = \hbar v_0(p_x\sigma_z + f_m p_y\sigma_y) + \hbar v_0 mG_0/2I. \tag{11}$$

After performing yet another similarity transformation $M' = U_2^\dagger M U_2$ with

$$U_2 = \frac{1}{\sqrt{2}}\begin{pmatrix} 1 & 1 \\ -1 & 1 \end{pmatrix}, \tag{12}$$

we obtain the final result:

$$M' = \hbar v_0(p_x\sigma_x + f_m p_y\sigma_y) + \hbar v_0 mG_0/2I. \tag{13}$$

The only difference of the Hamiltonian in Eq. (13) from that in Eq. (1), other than a constant energy term, is that the group velocity of quasiparticles moving along the y direction has been changed from v_0 to $f_m v_0$ [23]. Thus, the electronic states near $\mathbf{k} = \mathbf{G}_m/2$ are also those of massless Dirac fermions but having a group velocity varying *anisotropically* depending on the propagation direction. Moreover, the group velocity along the y direction is *always lower* than v_0 [Eq. (10)] regardless of the form or magnitude of the periodic potential $V(x)$.

The eigenstate and the energy eigenvalue of the matrix M' are given by

$$\varphi_{s,\mathbf{p}} = \frac{1}{\sqrt{2}}\begin{pmatrix} 1 \\ se^{i\phi_\mathbf{p}} \end{pmatrix}'' \tag{14}$$

and

$$E_s(\mathbf{p}) = s\hbar v_0\sqrt{p_x^2 + |f_m|^2 p_y^2} + \hbar v_0 mG_0/2, \tag{15}$$

respectively, where $\phi_\mathbf{p}$ is the polar angle of the pseudospin vector $\mathbf{c}$ of $\varphi_{s,\mathbf{p}}$, which is parallel to $s(p_x\hat{x} + f_m p_y\hat{y})$. The spinor $\varphi_{s,\mathbf{p}}$, however, should not be confused with the one in Eq. (2) representing the sublattice degree of freedom, or with the one in Eq. (8). A double prime in Eq. (14) emphasizes this point.

The eigenstate $\psi_{s,\mathbf{k}}(\mathbf{r})$ of the original Hamiltonian H in Eq. (4) can be obtained by using Eqs. (5), (8), (12), and (14). Since the unitary transformations conserve the inner product between eigenstates, if a *generalized* pseudospin vector for the original Hamiltonian H in Eq. (4) is defined as the pseudospin vector of the transformed Hamiltonian M', i.e., $\mathbf{c}$, the scattering matrix elements between states of these new massless Dirac fermions due to long-wavelength perturbations are described by the generalized pseudospin in the same manner as those of the original massless Dirac fermions in pristine graphene are described with their pseudospin.

On the other hand, the group velocity vector $\mathbf{v}_g$ is parallel to $s(p_x\hat{x} + f_m^2 p_y\hat{y})$ [Eq. (15)]. Therefore, in general, the three vectors $\mathbf{p}$, $\mathbf{c}$, and $\mathbf{v}_g$ are not collinear (Fig. 1). However, it is obvious that if the wave vectors ($\mathbf{p}$) of two electronic states are aligned or antialigned to each other, so are their generalized pseudospin vectors, as in pristine graphene, resulting in a maximum or a zero overlap between the two states, respectively. If $V(x)$ is not an even function, the dispersion relation of the new massless Dirac fermions remains the same as Eq. (15), but a generalized pseudospin vector may not be defined [25].

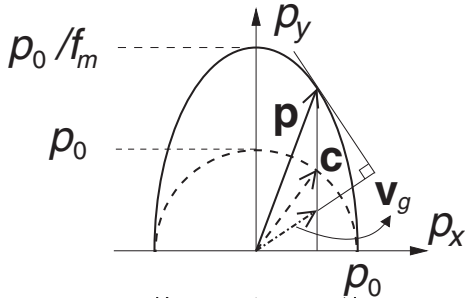

FIG. 1. Schematic diagram showing an equienergy contour (ellipse) with $E = \hbar v_0 k_0 + \hbar v_0 m G_0/2$ of the newly generated massless Dirac fermions. The quasiparticle wave vector $\mathbf{k}$, the generalized pseudospin vector (see text) $\mathbf{c}$, and the group velocity vector $\mathbf{v}_g$ are represented by solid arrows, dashed arrows, and dash-dotted arrows, respectively, for graphene in an even periodic potential.

Similarly, for graphene in slowly varying 2D periodic potential, new massless Dirac fermions are generated centered around the wave vectors $\mathbf{k}_c = \mathbf{G}/2$ where the $\mathbf{G}$'s are the superlattice reciprocal vectors. A state with wave vector $\mathbf{k}$ around $\mathbf{k}_c$ mixes strongly with another state with wave vector $\mathbf{k} - \mathbf{G}$ by the superlattice potential. Applications of the same argument that we made use of in the case of 1D graphene superlattices result in linear band dispersions.

Even though new massless Dirac fermions are generated in 1D graphene superlattices, because there is no SBZ boundary perpendicular to the periodic direction, they are obscured by other states, and there is no new value of energy at which the density of states vanishes. In 2D rectangular graphene superlattices, the SBZ is a rectangle. It turns out that the energy separation at the SBZ corners also vanishes due to the chiral nature of graphene [7]. Therefore, in 2D rectangular graphene superlattices, again, there are states other than the new massless Dirac fermions in the range of the new Dirac point energy. However, as we show below, in TGSs, there can exist an energy window within which the only available states are the newly generated massless Dirac fermions.

As an illustration, we consider a TGS shown in Fig. 2(a). The external potential is of a muffin-tin type with value U_0 in a triangular array of disks of diameter d and zero outside of the disks. The spatial period of the superlattice is L. Figure 2(b) shows the SBZ of a TGS.

Figure 2(c) shows the electron energy separation between states in the first and the second band above the original Dirac point energy along the path $\tilde{K}\tilde{M}\tilde{K}'$ in the SBZ [Fig. 2(b)] for a TGS. The energy separation at the corner, or the $\tilde{K}$ point, of the SBZ is largest, contrary to that of the rectangular graphene superlattices where the energy separation closes at the SBZ corners [7], but that at the $\tilde{M}$ point is zero. New massless Dirac fermions are thus formed

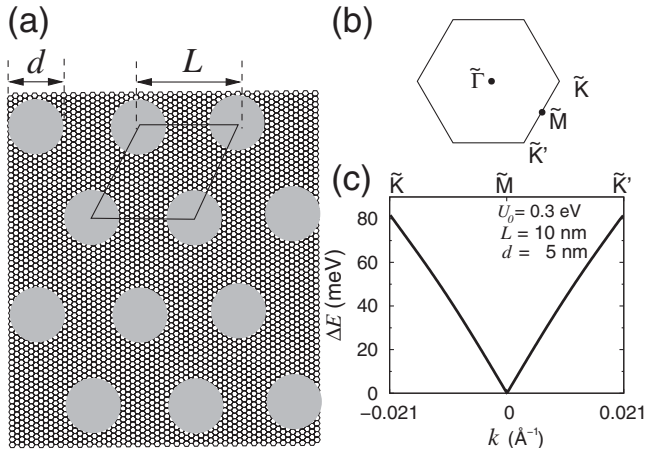

FIG. 2. (a) A TGS with muffin-tin type of periodic potential with a spatial period L. The potential is U_0 inside the gray disks with diameter d and zero outside. (b) The SBZ of a TGS. (c) The energy separation ΔE between states in the first and the second band above the original Dirac point energy versus the wave vector k along the path $\tilde{K}\tilde{M}\tilde{K}'$ in a TGS given by $U_0 = 0.5$ eV, $L = 10$ nm, and $d = 5$ nm.

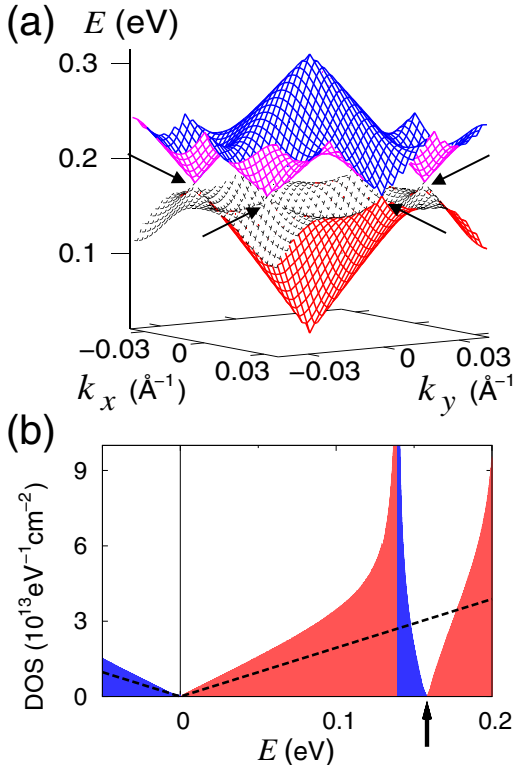

FIG. 3 (color online). (a) Energy dispersion relation of a TGS with external potential with $U_0 = 0.5$ eV, $L = 10$ nm, and $d = 5$ nm for the first and the second band above the original Dirac point energy as a function of wave vector $\mathbf{k}$ from the original Dirac point. Arrows indicate the $\tilde{M}$ points of the SBZ around which new massless Dirac fermions are generated. (b) The DOS of charge carriers in electron orbits (bright and red) and hole orbits (dark and blue) in the TGS characterized in (a). The original Dirac point energy is set at zero. Dashed black line shows the DOS of pristine graphene. The arrow indicates the new Dirac point energy.

around the $\tilde{M}$ points. With the set of potential parameters in Fig. 2 ($U_0 = 0.5$ eV, $L = 10$ nm, and $d = 5$ nm), the energy separation at the $\tilde{K}$ point is 82 meV, much larger than room-temperature thermal energy. This energy separation can be tuned by changing the superlattice parameters.

Figure 3(a) shows the energy dispersions of the first and the second band of the considered TGS. We can see the linear energy dispersion relation at the $\tilde{M}$ points [Fig. 2(c)]. Close to the original Dirac point energy ($E = 0$), the density of states (DOS) varies linearly with energy, similar to that of pristine graphene, except that the slope is larger because of the reduced band velocity. At around $E = 0.16$ eV, there exists another energy value where the DOS vanishes also linearly.

In conclusion, we have shown that a new class of massless Dirac fermions is generated in graphene when a periodic potential is applied and we have studied the novel characteristics of these quasiparticles. Moreover, in triangular graphene superlattices, there can exist energy windows where there are no other states than these new quasiparticles. The triangular graphene superlattices thus should provide a good platform for experimental probing of the new massless Dirac fermions predicted here.

C.-H. P. thanks D. S. Novikov for fruitful discussions. This work was supported by NSF Grant No. DMR07-05941 and by the Director, Office of Science, Office of Basic Energy Sciences, Division of Materials Sciences and Engineering Division, U.S. Department of Energy under Contract No. DE- AC02-05CH11231. Y.-W. S. was supported by KOSEF Grant No. R01-2007-000-10654-0 and by Nano R&D program 2008-03670 through the KOSEF funded by the Korean government (MEST). Computational resources have been provided by NPACI and NERSC.

Note added in proof.—After submission of this Letter, an angle-resolved photoemission experiment on graphene on Ir(111) surface resulting in superlattice formation was reported [26] in which minigap openings at the SBZ boundary are found and evidence of replicas of the primary Dirac cone observed.

*cheolwhan@civet.berkeley.edu

[1] R. Tsu, *Superlattice to Nanoelectronics* (Elsevier, Oxford, 2005).
[2] K. S. Novoselov *et al.*, Proc. Natl. Acad. Sci. U.S.A. **102**, 10 451 (2005).
[3] K. S. Novoselov *et al.*, Nature (London) **438**, 197 (2005).
[4] Y. Zhang, J. W. Tan, H. L. Stormer, and P. Kim, Nature (London) **438**, 201 (2005).
[5] C. Berger *et al.*, Science **312**, 1191 (2006).
[6] A. K. Geim and K. S. Novoselov, Nature Mater. **6**, 183 (2007).
[7] C.-H. Park *et al.*, Nature Phys. **4**, 213 (2008); C.-H. Park *et al.*, Nano Lett. **8**, 2920 (2008); M. Barbier, F. M. Peeters, P. Vasilopoulos, and J. M. Pereira, Jr., Phys. Rev. B **77**, 115446 (2008).
[8] F. Guinea, M. I. Katsnelson, and M. A. H. Vozmediano, Phys. Rev. B **77**, 075422 (2008).
[9] T. G. Pedersen *et al.*, Phys. Rev. Lett. **100**, 136804 (2008).
[10] D. Yu *et al.*, arXiv:0803.2660v1.
[11] J. C. Meyer, C. O. Girit, M. F. Crommie, and A. Zettl, Appl. Phys. Lett. **92**, 123110 (2008).
[12] S. Marchini, S. Günther, and J. Wintterlin, Phys. Rev. B **76**, 075429 (2007).
[13] A. L. Vazquez de Parga *et al.*, Phys. Rev. Lett. **100**, 056807 (2008).
[14] Y. Pan *et al.*, arXiv:0709.2858v1.
[15] T. Ando and T. Nakanishi, J. Phys. Soc. Jpn. **67**, 1704 (1998).
[16] P. L. McEuen *et al.*, Phys. Rev. Lett. **83**, 5098 (1999).
[17] P. R. Wallace, Phys. Rev. **71**, 622 (1947).
[18] We assume that appropriate constants are subtracted from $V(x)$ and $\alpha(x)$ so that the averages of $V(x)$ and $\alpha(x)$ are both zero.
[19] A similar transformation has been performed on the Hamiltonian of a carbon nanotube under a sinusoidal potential (Refs. [20,21]). In carbon nanotubes, a finite scattering probability along the periodic direction is given by a boundary condition along the circumferential direction, curvature, or magnetic field (Refs. [20,21]), whereas in graphene, the wave vector component k_y naturally serves the role of scattering along the periodic direction.
[20] V. I. Talyanskii *et al.*, Phys. Rev. Lett. **87**, 276802 (2001).
[21] D. S. Novikov, Phys. Rev. B **72**, 235428 (2005).
[22] If $V(x)$ is even, $\alpha(x)$ is odd [Eq. (6) and Ref. [18]]. If we take the complex conjugate of Eq. (6) and change x to $-x$, it is evident that $f_l[V]$'s are real.
[23] The matrix M' in Eq. (13) belongs to a generalized 2D Weyl Hamiltonian which has previously been employed to describe charge carriers in mechanically deformed graphene or possibly in an organic compound α-(BEDT-TFT)$_2$I$_3$ under pressure (Ref. [24]).
[24] M. Goerbig, J.-N. Fuchs, G. Montambaux, and F. Piechon, Phys. Rev. B **78**, 045415 (2008).
[25] If we remove the assumption that the periodic potential is an even function, Eqs. (11) and (13) read

$$M = \hbar v_0 \begin{pmatrix} p_x & -i f_m p_y \\ i f_m^* p_y & -p_x \end{pmatrix} + \hbar v_0 m G_0/2I$$

and

$$M' = \hbar v_0 \begin{pmatrix} -p_y \,\mathrm{Im} f_m & p_x - i p_y \,\mathrm{Re} f_m \\ p_x + i p_y \,\mathrm{Re} f_m & p_y \,\mathrm{Im} f_m \end{pmatrix} + \hbar v_0 m G_0/2I,$$

respectively. The energy eigenvalue of M' is given by Eq. (15). The eigenstate of M' corresponding to Eq. (14) is given by $\varphi_{s,\mathbf{p}} = \frac{1}{\sqrt{1+\lambda_{s,\mathbf{p}}^2}} (_{s\lambda_{s,\mathbf{p}} e^{i\phi_{\mathbf{p}}}}^{1})''$, where $\phi_{\mathbf{p}}$ is the polar angle of the vector $s(p_x\hat{x} + p_y \,\mathrm{Re} f_m \hat{y})$, and $\lambda_{s,\mathbf{p}} = [\sqrt{p_x^2 + |f_m|^2 p_y^2} + s p_y \,\mathrm{Im} f_m]/\sqrt{p_x^2 + p_y^2 (\mathrm{Re} f_m)^2}$. In general, $\lambda_{s,\mathbf{p}}$ is not 1, and, moreover, varies with the direction of $\mathbf{p}$.
[26] I. Pletikosic *et al.*, arXiv:0807.2770v1.